Geomorphic, sedimentary and hydraulic reconstruction of a glacial lake outburst flood in northern Alberta, Canada

SOPHIE L. NORRIS (iD), MARTIN MARGOLD, DANIEL J. UTTING AND DUANE G. FROESE

Glacial lake outburst floods occurred frequently during the last deglaciation of the Laurentide Ice Sheet. Within the Interior Plains, these floods carved large spillway systems; however, due to a lack of abundant sediment, deposits within prairie spillways are rarely preserved. Here, we present geomorphic and sedimentary evidence and hydraulic modelling of the eastern Beaver River Spillway, formed by the catastrophic drainage of the ice-dammed glacial Lake Algar, in north central Alberta. During this flood, coarse-grained sediment eroded from local till formed large pendant bars. Within the first ~50 km of the spillway (Reach 1), pendant bars contain downstream orientated foresets overlain by horizontally bedded coarser gravels. The remaining pendant bars (Reach 2), present downflow of a moraine barrier, differ, comprising massive, matrix-supported, inversely graded gravels capped by a boulder layer. We use a HEC-GeoRAS/HEC-RAS system in conjunction with palaeostage indicators to estimate the steady-state water surface elevation. Modelling results show that peak discharge within Reach 1 of the eastern Beaver River Spillway was approximately 14 000–21 000 $m^3 s^{-1}$. For Reach 2, 30 km downstream, the peak discharge was estimated at 23 000–40 000 $m^3 s^{-1}$ (n_{bulked} 18 000–26 000 $m^3 s^{-1}$). The downstream discharge increase, consistent with the sedimentary change in pendant bar deposits, is attributed to sediment bulking of the flood flow. This provides the opportunity to observe a range of flow conditions, and associated sedimentology, from a single flood event. The reconstructed flow conditions, coupled with lake volume estimates from the ponding above the moraine barrier suggest a minimum flow duration of 3–5 days.

Sophie L. Norris (e-mail: slnorris@ualberta.ca) and Duane G. Froese, Department of Earth and Atmospheric Sciences, University of Alberta, 1–26 Earth Sciences Building, Edmonton, AB, T6G 2E3, Canada; Martin Margold, Department of Physical Geography and Geoecology, Charles University, Albertov 6, 128 43 Praha 2, Czech Republic; Daniel J. Utting, Alberta Geological Survey, Alberta Energy Regulator, 402 Twin Atria Building, 4 4999-98 Avenue, Edmonton, AB, T6B 2X3, Canada; received 13th December 2018, accepted 20th April 2019.

Glacial lake outburst floods played a significant role in landscape evolution of the Interior Plains during deglaciation of the Laurentide Ice Sheet (LIS; Kehew 1982; Kehew & Lord 1986, 1987; Lord & Kehew 1987; Fisher & Smith 1994; Kehew & Teller 1994; Fisher *et al.* 2009; Fisher & Lowell 2017). Meltwater from the LIS, impounded by the region's reverse topographic slope, formed large interconnected systems of proglacial lakes draining across topographic thresholds and carving spillways. This resulted in the failure of unstable dams and outburst floods. The outburst floods frequently fed other topographically lower proglacial lakes, which in response also drained, producing a 'domino' like sequence of lake-drainage floods (Kehew & Clayton 1983). Flow during these catastrophic events was of high magnitude, short-lived and very erosive, carving spillways (Kehew & Lord 1986). Reconstructions of these events infer that the freshwater output from large glacial lakes associated with the LIS had the potential to cause abrupt changes in global climate via the disruption of ocean circulation patterns (Broecker *et al.* 1989; Clark *et al.* 2001; Fisher *et al.* 2002; Teller *et al.* 2002). Despite the existence of many spillways and the inferred broader impact of outburst floods, extensive sedimentary deposits are relatively rare, limiting palaeohydraulic reconstruction of flood deposits within the Interior Plains.

Here, we examine the sedimentology, geomorphology and palaeohydraulics of a catastrophic flood caused by the sudden drainage of an ice-dammed lake, glacial Lake Algar in north central Alberta (Fig. 1). We assess the nature and dynamics of the flood flow by analysis of the identified spillway and other well-preserved erosional and depositional features. We reconstruct the hydraulics of the outburst flood using a GIS based model and a digital elevation model (DEM) derived from shuttle radar topography mission (SRTM) data. Peak discharge is then inferred within a HEC-RAS model constrained by field evidence of the high water stage. We then assess the significance of this event in the context of both wider flood dynamics on the northern Plains, and the deglacial history of the region.

Regional setting

The modern-day Beaver River cuts through the Sand River, Cold Lake and Meadow Lake regions of Alberta and Saskatchewan, extending from its source (Beaver Lake, Alberta) ~240 km into northwest Saskatchewan. The river occupies a wide (0.2–0.9 km), deep (~40 m), steep-walled channel (herein referred to as the Beaver River Channel) (Fig. 1). A comparison of the modern-day river to the deeply incised channel suggests a considerably higher magnitude discharge was needed to explain its size and morphology (Dury 1976). The formation of the western portion of the channel has been attributed to the drainage of a large proglacial lake, glacial Lake Algar (Utting *et al.* 2015; Fig. 1). The
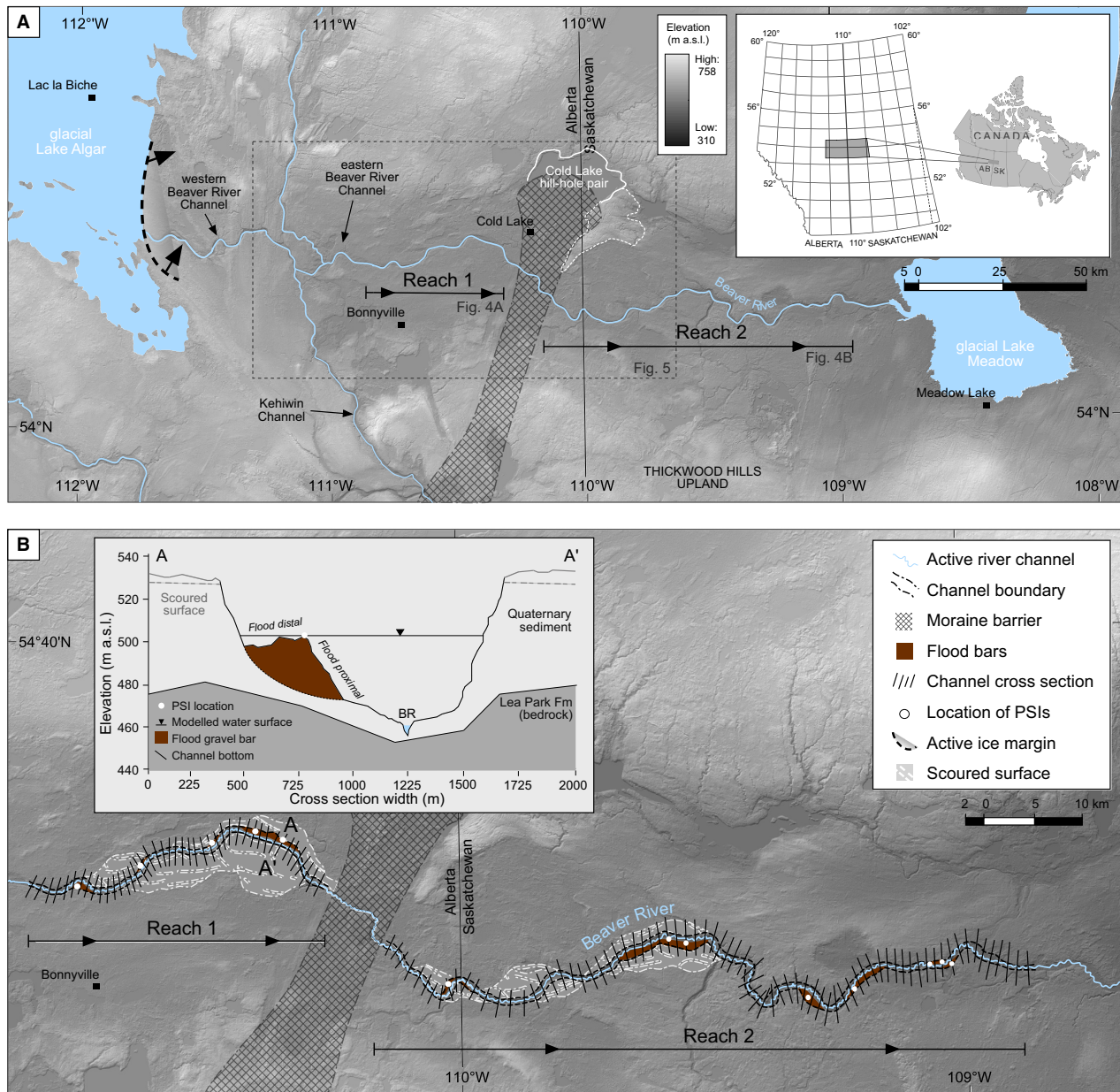
Fig. 1. A. Map of the study area showing the locations of modelled reaches in the Beaver River Channel. Flow direction is shown by the reach arrows. The maximum extent of glacial Lake Algar is shown west of the Beaver River Channel and glacial Lake Meadow to the east (from Utting *et al.* 2015). The locations of Figs 4A, B and 5 are marked. B. Step-backwater reach cross-sections. The locations of PSIs are indicated with white circles. Cross-sectional profile for A–A' is displayed as an inset diagram, showing the modelled water surface and deposited PSI. [Colour figure can be viewed at www.boreas.dk]

lake first drained to the east, forming the western portion of the Beaver River channel, after which the lake drainage became deflected southwards, through an ice-walled channel and into the Kehiwin Channel (Fig. 1).

While a clear formation mechanism for the western portion of the Beaver River Channel exists, to date only a brief mention of the eastern Beaver River Channel, as a meltwater channel feeding glacial Lake Meadow, between 13.9 and 13.3 ka BP (12–11.5 ^{14}C ka BP; Dyke *et al.* 2003), has been made (Christiansen 1979; Schreiner 1983; Andriashek & Fenton 1989). Furthermore, no explana-

tion has been proposed to adequately explain the size and morphology of the eastern portion of the channel. This portion of the Beaver River Channel is partially incised in predominantly thick, sand- and clay-rich glacial deposits (see Andriashek & Fenton 1989). In some areas, it has also incised through a thin veneer of sand and gravels that overlie the glacial deposits (Fig. 1). Approximately 50 km west of the Alberta/Saskatchewan border (Fig. 1), the channel dissects a ~10-km-wide area of streamlined and morainic terrain. This zone is dominated by hummocky mounds, lakes and flutings associated with an area of

localized fast ice flow, at its highest rising 10–12 m above the valley floor on either side (herein termed moraine barrier; see Fig. 1). Surrounding the channel the moraine barrier is heavily eroded to a distance of ~2.5 km on both sides. Built into the eastern portion of the Beaver River Channel, 12 gravel and sand deposits are visible. These deposits are large pendant bars that occur mostly at the inside of channel bends and constitute primary bedforms (Lord & Kehew 1987), mostly unmodified postdeposition.

Within the Canadian Prairies, morphologically and structurally similar deposits and landforms to those in the Beaver River region have been attributed to large subglacial meltwater events (e.g. Sjogren & Rains 1995; Munro-Stasiuk 1999; Beaney 2002). However, in contrast to these events the Beaver River Channel links two proglacial lakes, Algar and Meadow. Both lakes are demarcated by shorelines (Christiansen 1979; Schreiner 1983; Fisher & Smith 1994; Utting *et al.* 2015) and in the case of glacial Lake Meadow a delta occurs where the Beaver River Channel meets the lake. The geographical context for flood sediments and geomorphology in relation to a former ice margin is also clear. Multiple ice-marginal positions have been mapped (Utting *et al.* 2015), which deflect waters from glacial Lake Algar first to the south and then progressively retreating north of the Beaver River Channel. For these reasons, we consider it appropriate to interpret the channel morphology and sedimentology in the context of proglacial and marginal meltwater discharge.

Material and methods

Glacial lake outburst indicators

Channel morphology, erosional features, outburst flood deposits and the locations of palaeostage indicators (PSIs) were identified from a combination of in-field mapping, aerial photography, SRTM (1-arc, 30 m) and, where available, LiDAR (10 m) imagery. We use the crest of pendant bars as PSIs within the channel (Table 1). The location and elevation (m a.s.l.) of the PSIs were recorded using a hand-held GPS and loaded into ArcMap in order to utilize them in hydraulic modelling (see Table 1 for PSI summary). We consider these features to have formed rapidly during steady flow conditions that followed the initial flood wave subsequent to flood initiation. These PSIs thus provide a conservative estimate of peak discharge.

Where exposed, the internal structure of deposits was examined. The sedimentology of 16 exposures in 12 gravel pits was recorded with vertical profile logging or section sketches. Sediment particle (*b*-axis) measurements were taken at six gravel pits within the flood reaches (extensive aggregate excavation limited the measurement of *in situ* samples at all 12 bars). As not all particles (particularly boulder-sized clasts) were in their original depositional position, clast orientation was not measured; only the *b*-axis and roundness were recorded.

Step-backwater modelling

Pre-processing. – A one-dimensional, step-backwater method in conjunction with PSIs was employed in HEC-RAS (Horritt & Bates 2002) to model palaeoflood flow-behaviour. Topographic data for use in the hydraulic model were extracted from SRTM imagery. Incomplete spatial coverage meant LiDAR imagery was not utilized for the hydraulic modelling. Using HEC-GeoRAS 3.1 as an extension within ArcGIS 10.3, a total of 176 cross-sections were extracted from the DEM (spaced 750 m apart) along two sections of the channel.

Model development. – Using the established flow geometry and determined cross-sections, a steady state flow simulation in a 'mixed flow regime' mode produced a hydraulic reconstruction of the outburst flood for each of the two reaches. A water-surface elevation associated with peak discharge was then calculated by running the hydraulic model until the modelled water surface at respective cross-sections best matched the PSIs.

Flow energy losses are accounted for in HEC-RAS using coefficients for flow expansion and contraction and using a roughness coefficient (Manning's *n*). In accordance with previous outburst flood reconstructions (Herget 2005; Carling *et al.* 2010; Margold *et al.* 2018), to account for the uncertainty associated with assigning Manning's *n* values in a palaeoenvironment, a range of *n* values were used from 0.025 to 0.075. Predefined expansion and contraction coefficients of 0.1 and 0.3, respectively, were retained due to the uniform channel width in both reaches (Hydrologic Engineering Center 2001).

Table 1. Locations and elevations of PSIs along the Beaver River Channel.

PSI type	Latitude[1] (decimal deg.)	Longitude[1] (decimal deg.)	Elevation[1] (m a.s.l.)	Downstream distance in modelled reach[2] (km)
Pendant bar crest	54.3845	−110.7546	519	5.1
Pendant bar crest	54.4075	−110.6313	520	15.3
Pendant bar crest	54.4385	−110.4840	531	28.6
Pendant bar crest	54.4473	−110.4149	524	31.4
Pendant bar crest	54.4402	−110.3784	525	34.5
Pendant bar crest	54.2556	−110.0304	512	15.0
Pendant bar crest	54.3070	−109.5558	490	48.6
Pendant bar crest	54.3064	−109.5330	502	60.5
Pendant bar crest	54.2433	−109.2956	510	85.2
Pendant bar crest	54.2553	−109.2167	506	90.3
Pendant bar crest	54.2790	−109.0460	486	100.5
Pendant bar crest	54.2766	−109.0452	485	102.5
Pendant bar crest	54.2724	−109.0421	485	105.3

[1]Location and elevation of PSIs recorded in-field using a hand-held GPS.
[2]Downstream distance within HEC-RAS modelled reaches (Fig. 4).

Table 2. Predicted hydraulic variables from sediment particle b-axis calculations.

Reach location				Hydraulic parameter					
Lat. Long. (dd)[1]	Reach downstream distance (m)[2]	d_{max} $(d$, m)[3]	d_{50} $(d$, m)[4]	Costa (1983)			O'Connor (1993)		Ferguson (1994)
				Threshold velocity $(V_c$, m s^{-1}) $V_c = 0.18d^{0.49}$	Peak discharge $(Q$, m^3 s^{-1}) $Q = AV$		Threshold velocity $(V_c$, m s^{-1}) $V_c = 0.29d^{0.6}$	Peak discharge $(Q$, m^3 s^{-1}) $Q = AV$	Peak discharge $(Q$, m^3 s^{-1})
					Cross sectional area $(A$, m^2)	Q		Cross sectional area $(A$, m^2) Q	
Reach 1									
54.4075–110.6313	15.3	0.15	0.07	2.1	8745	18 000	1.5	8745 13 000	22 000
54.4061–110.6301	28.6	0.28	0.04	2.8	9639	27 000	2.1	9639 21 000	24 000
54.4477–110.4346	31.4	0.31	0.05	3.0	7994	24 000	2.3	7994 18 000	18 000
Reach 2									
54.2698–110.0260	15.7	1.66	0.40	6.8	9309	63 000	6.2	9309 58 000	270 000
54.3080–109.5453	61.2	1.40	0.37	6.2	14 615	92 000	5.6	14 615 82 000	260 000
54.2604–109.2072	90.6	1.52	0.29	6.5	11 906	77 000	5.9	11 906 70 000	150 000
54.2792–109.0458	102.5	1.30	0.25	5.8	10 007	60 000	5.3	10 007 54 000	140 000

[1]Location and elevations recorded in-field using a hand-held GPS.
[2]Downstream distance within HEC-RAS modelled reaches (Fig. 4).
[3]Refers to the mean of the *b*-axis measured from the five largest clasts found *in situ* at each site.
[4]Refers to the median grain size of the 100 measured clasts.

Local hydraulic variables derived from particle diameter

To provide a comparable independently derived calculation of key hydraulic variables (velocity and peak discharge) used in step-backwater modelling, variables were also derived from the intermediate (*b*-axis) diameter of the five largest sediment particles at each bar (d_{max}) (Costa 1983; Williams 1983; Komar 1987; O'Connor 1993; Ferguson 1994). Only the five largest *in situ* sediment particles were measured to avoid underestimating hydraulic variables, as smaller sediment particles on the bar surface may have been deposited during lower discharges subsequent to peak discharge (O'Connor 1993).

Empirical relationships for determining hydraulic variables in this way have been derived by multiple authors. Only those data sets that incorporate a range of particle diameters concordant with those observed in the Beaver River Channel are applied (Costa 1983; Komar 1987; O'Connor 1993; Ferguson 1994; Table 2).

Following Costa (1983), velocity can be estimated by:

$$V_c = 0.18d_{max}^{0.49} \qquad (1)$$

where V_c = threshold velocity, and d_{max} is mean of the *b*-axis of the five largest sediment particles in mm.

An alternative regression-derived function is provided by O'Connor (1993):

$$V_c = 0.29d_{max}^{0.6} \qquad (2)$$

where V_c = threshold velocity, and d_{max} is mean of the *b*-axis of the five largest sediment particles in cm.

Using the relationships derived by Costa (1983) and O'Connor (1993) discharge along the Beaver River Channel was estimated using the continuity equation:

$$Q = AV \qquad (3)$$

where Q = discharge (m^3 s^{-1}), A = channel cross-sectional area (m^2) and V = mean flow velocity (m s^{-1}).

The final method for determining discharge (critical unit discharge p_c) is provided by Komar (1987) as reworked by Ferguson (1994). This method is based on the principle that on a bed of mixed clast sizes flow competence is a function of clast size relative to the median diameter of the deposit as a whole:

$$q_c = a\,d_{50}^{1.5}(d_{max}/d_{50})^{(1-x)(c+1.5)}/S^{(c+1)} \qquad (4)$$

$$\text{where } a = m(8g)^{0.5}((p_s/p - 1)\tau_{c*50})^{c+1.5} \qquad (5)$$

where d_{50} is the median grain size of a sample of 100 clasts at each site (see Table 2), S is the local channel gradient (m m^{-1}), p_s is the density of clasts (2650 kg m^{-3}), p is the density of water at 4 °C (1000 kg m^{-3}), g is gravitational acceleration, x is the hiding factor ($x = 0.9$; Parker 1990), m and c are constants related to a specified flow resistance relationship ($c = 0.37$, $m = 1.14$; Thompson & Campbell 1979), and τ_{c*50} is the critical dimensionless shear stress (0.045).

Results

Channel morphology and outburst deposits

Scoured surfaces and inner channel. – Based on in-field observations and LiDAR/SRTM imagery reviewed in

ArcMap, the Beaver River Channel comprises two major sections: a deep inner channel and a scoured outer surface. The deep (~40 m) inner channel is wide (0.2–0.9 km) and flat-bottomed. The channel has steep walls, and isolated coarse gravel deposits (pendant bars) that form intermittent terraces along its length. Outburst sediments are not visible along the bottom of the inner channel. The scoured surface is discontinuous and occurs typically at pendant bar locations. These surfaces are often capped by a littering of boulders with a *b*-axis of 0.7–2 m.

The largest area of scoured surface occurs immediately west of the ~10-km-wide moraine barrier (Fig. 1). Here a ~4-km-wide area of isolated scoured surfaces is dissected by shallow (1–3 m deep) anastomosing channels. Borehole logs from the scoured surface (AGS-SRT-11 (latitude 54.3624°N, longitude 110.6307°W), AGS-SRT-6, (54.4131°N, 110.4366°W), AGS-SRT-30 (54.3404°N, 110.4051°W)) comprise ~4 m of sorted sands and gravel overlying >50 m of sandy or clay-rich diamict.

Pendant bars. – Based on mapping from LiDAR/SRTM imagery, 12 pendant bars are visible within the Beaver River Channel (Fig. 1). Pendant bars, mostly unmodified by erosion, have been deposited most often at the inside of channel bends. Bars form terraces, with a gentle reverse distal slope leading to a steep proximal face (Fig. 1). Average bar dimensions are 2 km long, 0.5 km wide and 20 m thick.

The sedimentological characteristics of pendant bars can be characterized as two distinct groups (summarized in Fig. 3). Pendant bars in the first 40 km (Reach 1; Fig. 1) of the eastern Beaver River Channel, upflow of the moraine barrier, consist of 4–7 m of large-scale cross-bedded downstream directed gravels interspersed with granular and coarse sand beds. In the proximal portions of these bars this unit is overlain by horizontally bedded coarser gravels (Figs 2A, 3A). The petrology of gravels is varied, with an abundance of metamorphic and igneous rocks within the largest fraction. Rip-up clasts are also interspersed within the gravels. These clasts are recorded (although infrequently) at all gravel bars, and range in diameter from 7 to 30 cm. Rip-up clasts contain clay-rich diamict, occasional pebbles and exhibit a thin armour of coarse gravels.

Large-scale crude cross-bedding in the proximal portions of bars exhibits medium to thick (30–60 cm) beds of poorly sorted, silt to cobbles (>20 cm in diameter) with a dip of 10–20° (Figs 2A, 3A). At these locations, cross-beds grade into 2–2.5 m of horizontally bedded (30–100 cm) coarser gravels (maximum clast size of 20–30 cm). Maximum clast size within the horizontally bedded gravel unit decreases downstream between bars within the 40-km reach. Away from proximal zones, cross-beds are thinner (>50 cm thick) and fine away from the main channel, comprising clasts with a maximum diameter >15 cm (Figs 2B, 3B). At some of these locations, a 20–30 cm unit

of thin (<10 cm) cross-bedded sands overlie the gravels, although this unit is not present at all bars (Fig. 3B).

A 1–1.5 m unit of thinly laminated sand, silt and clay caps gravels in the most distal portion of one pendant bar (Figs 2C, 3B). This unit typically consists of rhythmically bedded sand/silt and clay-silt couplets. Individual couplets are 2–15 cm thick with the clayey-silt layer constituting 10 cm of the couplet. Thicker couplets contain climbing ripples as well as soft sediment deformation structures (flames and ball-and-pillow structures; Figs 2D, 3B). It should be noted that in two places this unit is overlain by a thin >50-cm diamict. However, based on its sporadic occurrence and the considerable aggregate excavation it seems highly unlikely the diamict is in place, but is instead the result of ongoing land reclamation on this pendant bar. If the diamict at the section interpreted as moved into place during aggregate excavation is in fact *in situ* till, the sediments composing this pendant bar would be an erosional remnant that was deposited in a pre-last glacial channel, overridden by the glacier ice and subsequently incised by the present channel.

Within the remaining 120 km of the eastern Beaver River Channel (Reach 2; Fig. 1) pendant bars differ sedimentologically (Fig. 3). The proximal zones of individual bars comprise massive, inversely graded, matrix-supported cobble and boulder gravels (up to 1–2.3 m in diameter; Figs 2E, 3C). Coarser clasts are weakly imbricated, but the gravels are otherwise structureless. Gravels are sedimentologically identical to that described above and rip-up clasts are also present, although in much higher frequencies and often larger in diameter (10–50 cm). The composition of the bars is nearly identical in appearance from one bar to another; however, within a single bar gravels fine markedly away from the main channel, i.e. from proximal to distal (Fig. 3C, D).

In the distal portions of these bars finer grained gravels (30 to 120 mm) containing cross-stratification and lenses of horizontally stratified sands and fine gravels are present (Fig. 3D). In some places, a thin 5–10 cm unit of planar cross-bedded sands overlies the gravels. However, at the majority of bars this unit is not present and the surface of bars, especially at their proximal portions, is covered with a littering of boulders (Fig. 2F).

Hydraulic analysis

Step-backwater modelling was performed for Reach 1 (40 km) and Reach 2 (120 km) of the eastern Beaver River Channel (see Fig. 1 for reach locations). These sections of the channel were selected for their high PSI density and minimal flow irregularities. Step-backwater calculations for these reaches provide discharge estimates that closely coincide with PSI evidence at modelled minimum discharges of 14 000–21 000 m^3 s^{-1} (Reach 1) and 23 000–40 000 m^3 s^{-1} (Reach 2) based on a Manning's *n* range of 0.025–0.075 (minimum peak discharge rounded to the nearest 500 m^3 s^{-1} at which pendant bars are submerged)
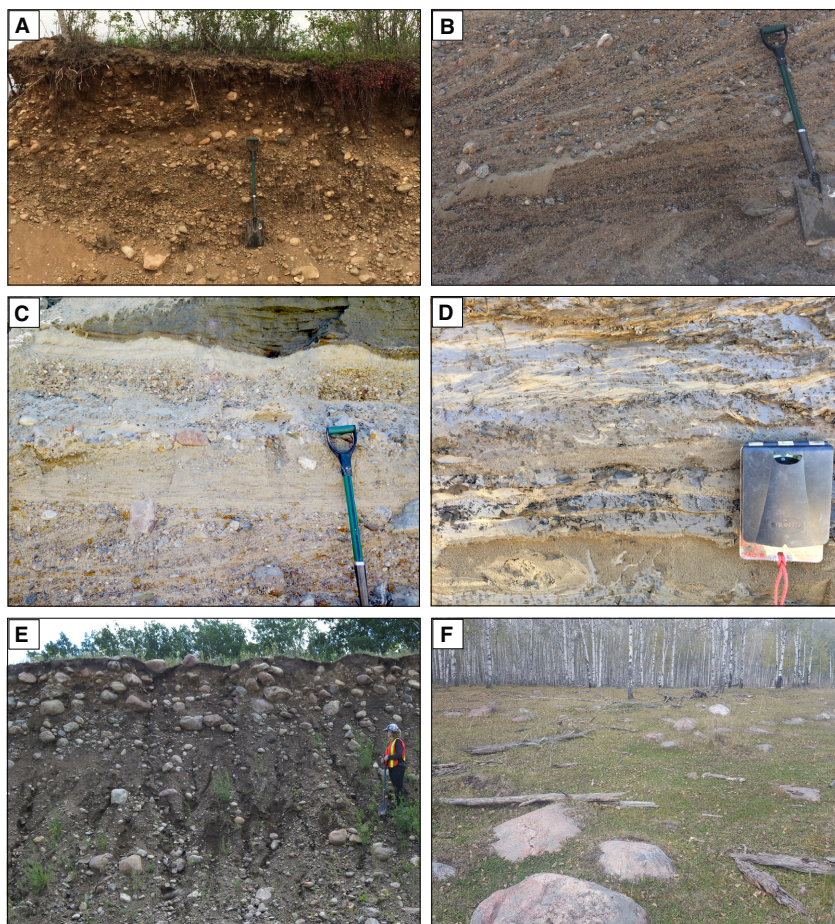
Fig. 2. Flood deposits observed at pendant bars along the Beaver River Channel. A. Exposure from a gravel pit on the proximal portion of a pendant bar (54.4073°N, 110.6313°W) located upstream of the moraine barrier. Clast-supported gravels with downstream directed cross-bedding overlain by coarse horizontal bedded gravels. Direction of flow is from left to right. B. Thinner cross-bedded gravels and sands on the distal portion of a pendant bar (54.4421°N, 110.3785°W), upstream of the moraine barrier. C. Cross-bedded gravels interspersed with granules and coarse sand beds unconformably overlain by ripple cross-laminated sand, silts and clays (54.4422°N, 110.3780°W). D. Ripple cross-laminated sand, silts and clays with soft-sediment deformation structures (flames and ball-and-pillow structures) (54.4402°N, 110.3713°W). E. Massive, matrix-supported, inversely graded boulder gravels (54.2541°N, 109.2164°W). Coarse clasts are weakly imbricate indicating flow from right to left. F. Littered boulders on the surface of a pendant bar 30 km downstream of the moraine barrier (54.2781°N, 109.0456°W). For scale horizontal tree trunk is 1.4 m long. [Colour figure can be viewed at www.boreas.dk]

(Fig. 4). Within Reach 1 the fit was good (±4 m) within all sections of the reach. Within Reach 2 the fit was good (±5 m) within the upper 75 km of the modelled reach, whereas within the lower 45 km this discharge produced a water surface 3–4 m below the PSI evidence. Nevertheless, the best-fit water surface was achieved with a 23 000–40 000 $m^3 s^{-1}$ peak discharge.

In addition to step-backwater modelling within HEC-RAS, we applied three empirical equations to independently calculate key hydraulic variables from sediment particle *b*-axis data. Within Reach 1, empirical equations yield hydraulic variables (velocity and peak discharge) in the same order of magnitude as those obtained from HEC-RAS modelling (Table 2). In contrast, within Reach 2 hydraulic variables show large discrepancies. These values show on average a fourfold increase compared to those derived from HEC-RAS.

Interpretation

Channel morphology

Based on comparison of previously reported spillways whose origin has been linked with known catastrophic lake drainage (e.g. Malde 1968; Baker 1973; Kehew & Lord 1986; Lord & Kehew 1987; Maizels 1991; Kehew 1993; O'Connor 1993; Cutler *et al.* 2002; Fisher & Taylor 2002; Kozlowski *et al.* 2005), we interpret the (eastern) Beaver River Channel as a spillway (herein referred to as the Beaver River Spillway) formed by catastrophic flood drainage. Evidence for this interpretation includes: (i) a steep walled, trench-like channel morphology; (ii) the occurrence of large (pendant) bars; and (iii) regions of erosional/scoured sub-upland/terrace.
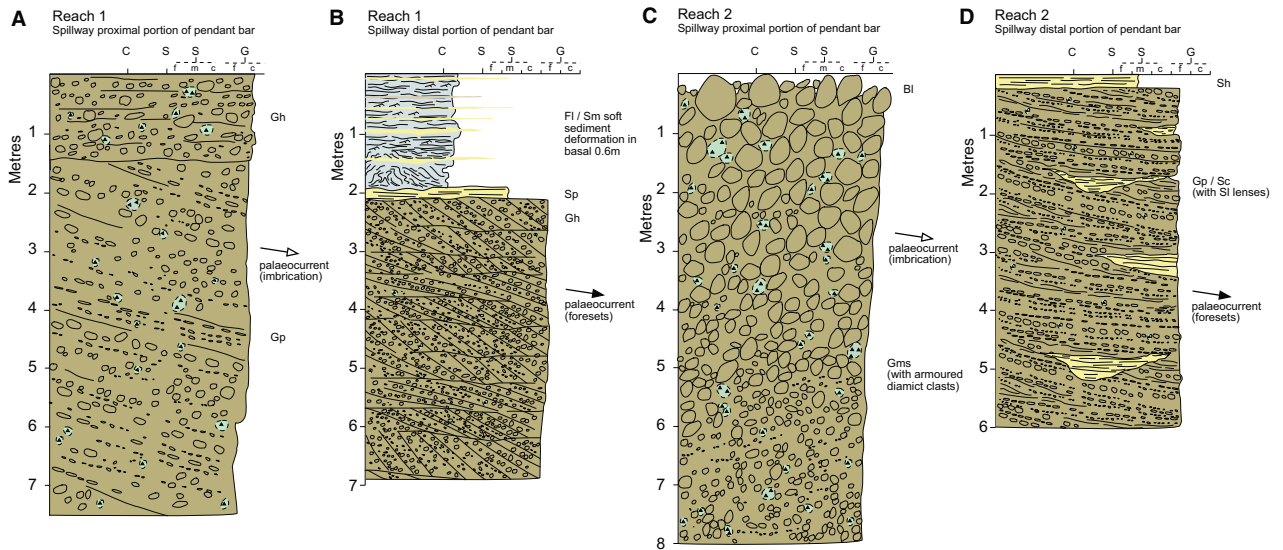
Fig. 3. Summary stratigraphical logs for Reach 1: spillway proximal (A) and distal (B) portions of pendant bars; and Reach 2: spillway proximal (C) and distal (D) portions of pendant bars. Fl/Sm = fine laminations of silt and clay with small ripples and minor fine sand/massive sands; Sp = medium to coarse planar crossed-bedded sands; Gh = horizontally bedded medium to coarse grained gravel; Gp = planar crossed-bedded gravel; Sh = horizontally bedded sands; Gp/Sc = planar cross-bedded gravel/ planar cross-bedded sands; Sl = horizontally laminated sand (lenses); Bl = boulder lag; Gms = matrix-supported, massive gravel. [Colour figure can be viewed at www.boreas.dk]

We interpret the scoured surfaces as characteristic of initial downcutting by floodwater where a deep valley system had not yet evolved. The scoured surfaces bear resemblance to the 'Outer Scour Zone' described by Kehew & Lord (1986). In their model, the Outer Scour Zone represents the initial stages of erosion, when no channel of sufficient size was available to convey the flood, and water covered a broad area (covered by anastomosing channels). Boulders exposed on the scoured surface were probably exhumed by erosion during channel incision, which promoted washing of finer surface sediment downstream, leaving coarser clasts exposed at the surface

(Kehew & Lord 1986). As flow continued, erosional enlargement concentrated within a smaller cross-sectional area began to erode the inner channel. Geomorphic and stratigraphical relations along the eastern Beaver River Spillway conform to this model. Here, the scoured surfaces are expansive and contain small channels making this initial flood zone inefficient because of its large wetted perimeter, leading to the progressive development of the trench-like main spillway channel (Kehew & Lord 1986). In addition to the large wetted perimeter, the boundary resistance to flow progressively increased within the scoured surface, with the development of the observed
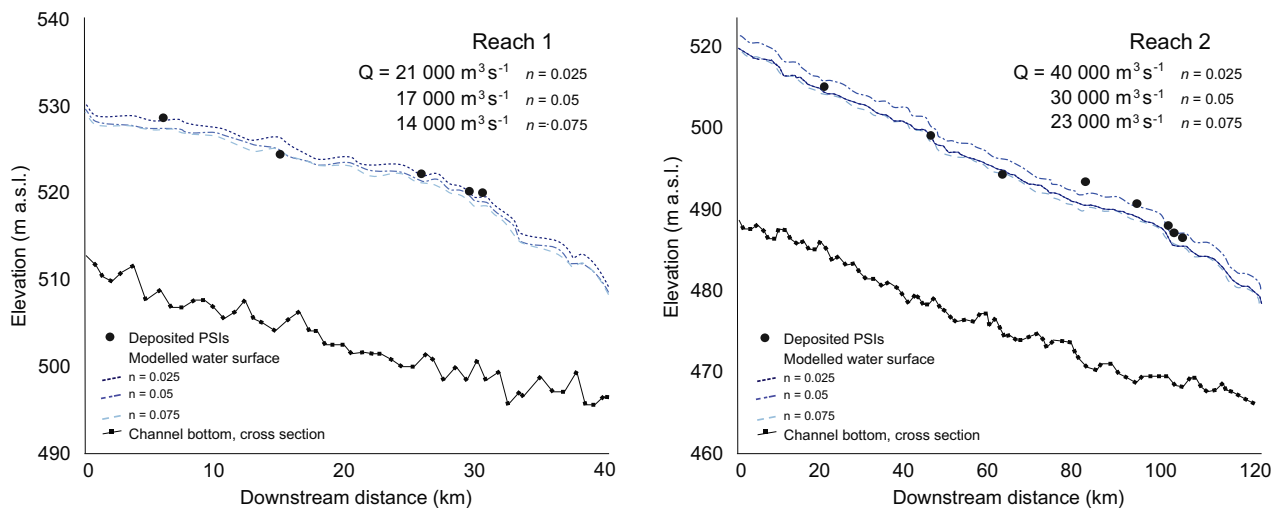

Fig. 4. HEC-RAS water-surface profiles and comparison with PSIs at modelled, maximum discharges of 14 000–21 000 and 23 000–40 000 m³ s⁻¹ for Reach 1 and 2, respectively. [Colour figure can be viewed at www.boreas.dk]

boulder lag, quickening the formation of a deep, narrow inner channel (Kehew & Lord 1986; Maizels 1997).

Outburst deposits and depositional processes

Pendant bars recorded in Reach 1 of the eastern Beaver River Channel, upflow of the moraine barrier resemble in form, although are smaller in size than those produced by Pleistocene Lake Bonneville catastrophic floods (Malde 1968) and Lake Missoula (Baker 1973; O'Connor 1993). Their internal structure is also similarly composed of downstream orientated foresets overlain by horizontally bedded coarser gravels (Fig. 3A). The formation mechanism of Baker (1973) and O'Connor (1993), in which bars grow as material transported as bedload across the surface of a bar is deposited on the downstream side, is invoked to explain these deposits. This sequence therefore reflects deposition by a single (fluid flow) flood not considerably deeper than the bar surface. Smaller scale cross-bedding and sediment fining in the flood distal portion of pendant bars are consistent with such a model and indicate regions of lower velocity further from the main channel (Carling 2013).

Thinly laminated sand, silt and clay cap gravels in the most distal portion of one pendant bar (Figs 2C, 3B). Similar deposits have been interpreted as slackwater deposits (Bretz *et al.* 1956; Waitt 1980, 1985; O'Connor *et al.* 2001). In our study, however, due to the localized nature of these deposits we simply interpret them to have formed in an area of flow stagnation or quiescence in the distal portion of a bar adjacent to the high energy floodway.

The remaining pendant bars, present downflow of the moraine barrier, exhibit differing internal structure containing no cross-stratification and considerably larger boulder clasts (Fig. 2C, D). Such deposits are more akin to those described by Lord & Kehew (1987) and Kehew & Lord (1987) in the Souris Spillway, and by Kozlowski *et al.* (2005) in the Central Kalamazoo River Valley, consistent with a type F5 vertical sedimentary profile (Maizels 1997). Massive, matrix-supported, inversely graded gravels capped by a boulder layer in these studies have been inferred or documented to be the product of an intermediary flow between debris and fluid flow termed hyperconcentrated (40–70% sediment concentration by weight; Costa 1984; Lord & Kehew 1987). In such flows, boundary shear stress can travel through the flood flow as a dispersive pressure, forcing coarse grains to move to the edges of the channel where shear is lower, thus producing inversely graded sequences with larger boulder sized clasts left as an armoured surface (Fig. 2F; e.g. Pierson 1981; Smith 1986; Maizels 1997; Carling 2013).

Armoured rip-up clasts comprised of till occur frequently in pendant bars downflow of the moraine barrier. It is possible that rip-up clasts were dislodged/eroded from frozen ground and were transported into place by the proposed hyperconcentrated flow. The higher frequency of such clasts in these pendant bars, compared to those upstream of the moraine barrier, attests to such an interpretation as rip-up clast moving by saltation or rolling, would be more easily broken down (Fisher 1993). It should be noted, however, that while the presence of such clasts has been previously described as diagnostic of subglacial excavation (Russell *et al.* 2006), based on the clear proglacial setting of this flood (see above) we suggest that such features cannot be used as indicative of a subglacial setting.

In the distal portions of bars, upflow of the moraine barrier, finer grained gravels containing indistinct cross-stratification and lenses of stratified sands and fine gravels are present (Fig. 2D). The presence of such deposits is characteristic of fluid flow and, therefore, indicates a lateral transition within the flow. Todd (1989) reports similar lateral transition in a flood flow associated with sediment bulking, where the basal portion of a flow moves as a hyperconcentrated flow while the upper and distal portions exhibit fluid flow characteristics. This interpretation is favoured in the Beaver River Spillway due to the sedimentary variation within a single pendant bar.

Comparison of modelling results to channel deposits

Comparison of local hydraulic variables (velocity and peak discharge), derived from the step-backwater modelling and from the *b*-axes of the 5 largest sediment particles within Reach 1, shows good agreement (Table 1). In contrast, within Reach 2 values derived from *b*-axis measurements are considerably (average fourfold increase in peak discharge) higher. Previous studies acknowledge (Lord & Kehew 1987; O'Connor 1993) the relationship between particle diameter and indices of flow may be overestimated. Data sets from which this relationship is derived may include samples not related to peak discharge but rather samples deposited during lower discharge after peak discharge (see O'Connor 1993 for review). However, it is doubtful this would create changes large enough to explain the discrepancy observed here. Alternatively, these overestimates are more likely the result of high sediment concentrations (Lord & Kehew 1987) within Reach 2. As indicated above, and based on the sedimentary observation (Fig. 3C, D) these flows would have been hyperconcentrated. Such concentrations may have lowered the shear stress needed to transport boulders (1.33–1.66 m) by altering the viscosity of the flow (Lord & Kehew 1987). Thus palaeohydraulic calculations made assuming a Newtonian fluid result in unrealistically large values.

Discussion

Palaeohydraulic reconstruction

The step-backwater modelling of the Beaver River flood allows hydraulic variables in the flood path to be compared and associated with field evidence. From this

modelling, we estimate peak discharge achieved along the eastern Beaver River Spillway was 14 000–21 000 m^3 s^{-1} upstream of the moraine barrier and 23 000–40 000 m^3 s^{-1} subsequent to it. There is a good agreement, (>±4, 6 m Reach 1 and 2, respectively) between flood geomorphology (PSIs) and hydraulic variables derived in HEC-RAS in both reaches (Fig. 4).

Hydraulic variables derived from the *b*-axis of the five largest boulders recorded at multiple pendant bars provide independent verification of HEC-RAS results. Within Reach 1 hydraulic variables derived from the two methods are consistent. In contrast, overestimated values were produced in Reach 2 when hydraulic variables were derived from *in situ* boulders. Based on the lack of association between boulder diameter, indices of flow and supporting sedimentological evidence, it is hypothesized that within this 120-km portion of the spillway the sediment concentration (and also the volume) and therefore its peak discharge increased. By comparison in Reach 1, in the 40 km more proximal to the flood source, transported large boulders are lacking and the sedimentological evidence is consistent with 'normal' fluid flows. Such a relationship is in contrast to proposed models of glacial lake outburst floods where gradual reduction in suspended sediment concentration in hyperconcentrated flows as the outburst flood propagates downstream can lead to the development of Newtonian flow dynamics (Maizels 1991; Maizels 1997). These characteristics signify a more complex system operated in the Beaver River channel.

Based on the assumption of a hyperconcentrated flow, the limitations of using a 1D steady state HEC-RAS model should also be discussed. This modelling approach assumes that a sediment enriched flow can be modelled as a Newtonian fluid in which the mass and density remain unchanged. This approach is unlikely to be valid when applied to a higher concentration debris flow; however, the method may provide a reasonable estimate for the hydraulic dynamics of a dilute hyperconcentrated flow when properly calibrated (Travis *et al.* 2012). Due to the low gradient of the slope we would expect a fluid flow enriched with sediment to travel at a lower velocity than a traditional fluid flow, thus the peak discharge derived in this study for Reach 2 may be overestimated and should be treated as a maximum estimate.

To account for this overestimate of velocity and provide a more accurate peak discharge range, a small number of studies have suggested that HEC-RAS input parameters be altered in order to account for the higher viscosities and densities of hyperconcentrated flows (Travis *et al.* 2012). The principle of this approach alters the normal parameters (expansion and contraction coefficients and Manning's *n*) to experimentally determined 'bulked' parameters that account for the bulked flow effects (Travis *et al.* 2012). This provides a more realistic reconstruction of flow conditions consistent with sedimentological evidence of hyperconcentration.

Following Travis *et al.* (2012) expansion/contraction coefficients and Manning's *n* can be recalculated allowing a peak discharge to be modelled in HEC-RAS. Using these new values, a peak discharge range of 18 000–26 000 m^3 s^{-1} is estimated. However, this range probably provides an upper estimate of peak discharge as it assumes the whole water column has a single 'bulked' viscosity.

Formation of the Beaver River Spillway

The following series of events (summarized in Fig. 5) are proposed to explain the geomorphic, sedimentary and hydraulic evidence observed in the Cold Lake/Meadow Lake region. During ice retreat to the northeast, and resulting from the regional reverse topographic slope, multiple proglacial lakes developed (Utting *et al.* 2015). Regionally, the largest of these lakes was glacial Lake Algar, which drained to form the westerly part of the Beaver River Spillway. Due to an ice margin inhibiting drainage to the eastern part of the Beaver River Spillway, water was instead deflected south travelling through an ice-walled channel into the Kehiwin Channel (Fig. 5A) (Utting *et al.* 2015).

Based on the juxtaposition of this ice-walled channel and a series of subaerial channels that has been eroded into progressively lower topography, we propose that as the ice margin retreated from its initial position (Fig. 5A), and/or discharge from glacial Lake Algar increased, the southern deflection of flood waters no longer occurred or was significantly reduced. Instead the flood progressively travelled in a more easterly direction to form the remaining eastern Beaver River Spillway. As water began to flow east towards the Alberta/Saskatchewan border, the ice margin would have been positioned north of the Beaver River Spillway. Evidence for this has previously been recognized by Andriashek & Fenton (1989) in terms of a ~12-km-wide belt of glacially compressed and thrusted landforms (Fig. 5B) extending from Barbara Lake eastward to Cold Lake. Prior to ice retreat to this

Fig. 5. Reconstructed development sequence for the Beaver River Spillway. A. Initial southeastward drainage of glacial Lake Algar along the western Beaver River Spillway. Water would have initially flowed through an ice-walled channel before entering the Kehiwin Channel. Easterly retreat of an ice lobe covering the lower Beaver River region allowed drainage in a progressively easterly direction through a network of meltwater channels. B. Continued northeastward retreat of ice allowed water to flow eastward, moraine barrier would then have blocked further eastward drainage and formed a short-lived ponded region. C. Once the water level overtopped the moraine barrier, progressive erosion of the spillway on both sides of the barrier occurred. Inset diagram shows the geomorphic imprint of the scoured surfaces and inner spillway channel. [Colour figure can be viewed at www.boreas.dk]
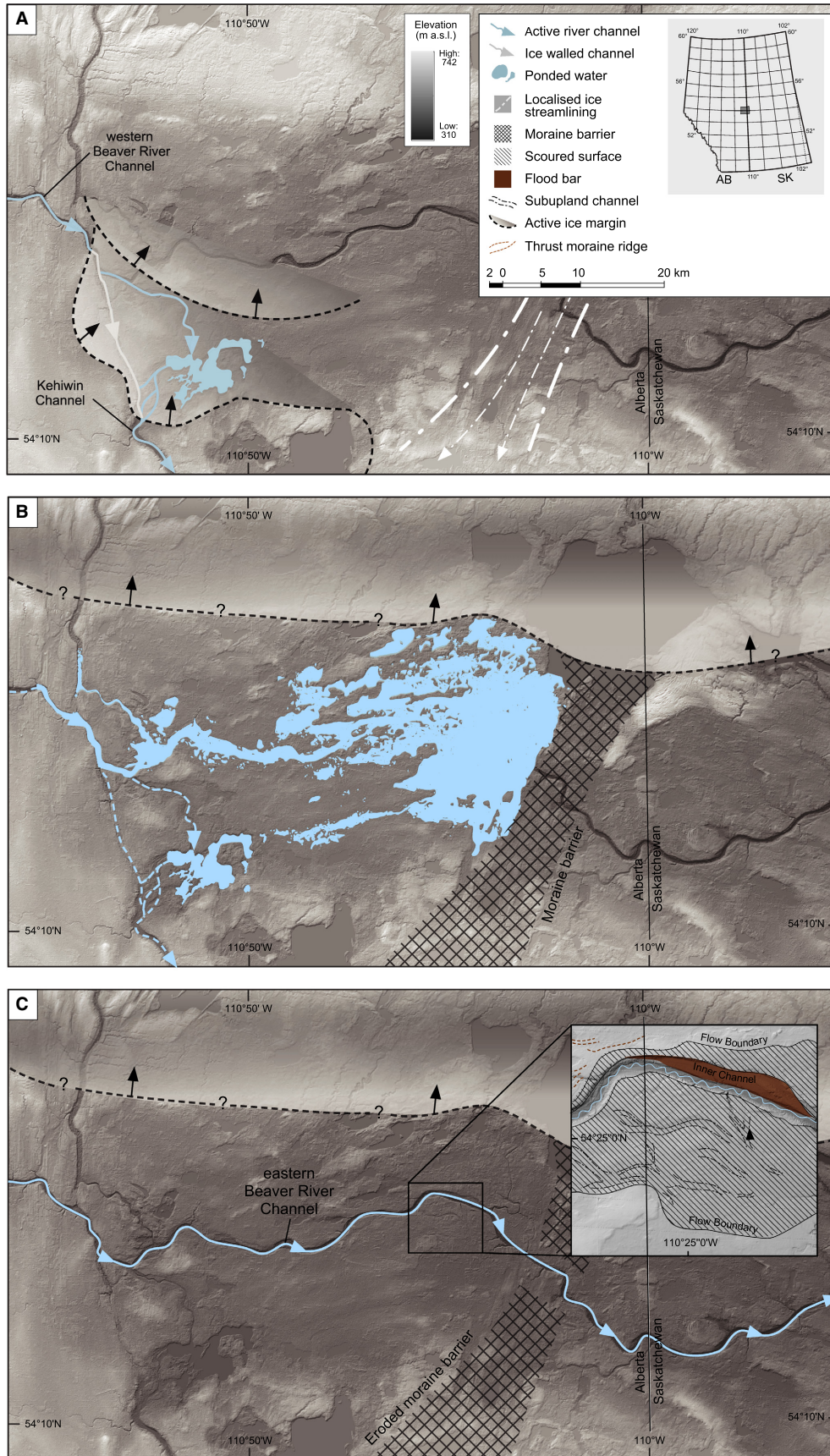
position a ~10-km-wide, localized area of streamlined, and morainic topography developed (the moraine barrier). This moraine barrier has previously been attributed to an ice re-advance extending southwest from Cold Lake ~80 km (Andriashek & Fenton 1989). However, due to the very small width and significant length of the terrain zone, we suggest this topography was instead formed by local fast ice flow, which may have been initiated by the large amount of glaciotectonized material available immediately north (i.e. the Cold Lake hillhole pair; Fig. 1). As flood flow travelled eastward it was impounded by this moraine barrier. As a result, flood water would have been temporarily impounded west of the moraine barrier. A thin veneer of sands and gravels, potentially of glaciolacustrine origin, supports this suggestion (Andriashek & Fenton 1989). Based on the elevation of morainic deposits surrounding the spillway, the impounded water spanned an area of 554 km^2 with an elevation of 540 m a.s.l. and volume ~5.5 km^3. A larger volume could not have been sustained above this elevation as water would have drained to the south via the Kehiwin Channel. Only once the water level was such that it could overtop the moraine barrier, would flood flow have started cutting across the region. The initial breach would have then deepened and widened to produce a ~2.5-km region of eroded streamlined terrain/moraine on both sides of the Beaver River Spillway.

As flood flow progressed through the region, it would initially have been largely unconfined, covering a region equivalent to the areas of scoured surfaces, travelling first as sheetflow and evolving to a progressively more channelized system. As flow continued, erosional enlargement concentrated within a smaller cross-sectional area would have then begun to erode the inner spillway (Kehew & Lord 1986). Prior to the moraine barrier flow would have had Newtonian characteristics. This type of flow was evidenced by well-preserved sedimentary evidence, downstream orientated foresets overlain by horizontally bedded coarse gravels, and the consistency between hydraulic variables derived empirically from particle diameter and from HEC-RAS. As this flood flow travelled through the easily erodible moraine barrier, it would have drastically increased its abundance of sediment by weight. This produced matrix-supported, inversely graded gravels capped by a boulder layer indicative of a hyperconcentrated flow. Additionally, this sediment-rich flow also produces erroneously high peak discharges when modelled as a Newtonian fluid.

In contrast to many spillways within the Interior Plains where deposits are absent, the eastern Beaver River Spillway displays an excellent sedimentary record. The path of the Beaver River Spillway cuts through thick sand- and clay-rich glacial deposits, commonly >50 m thick (Fig. 1). We suggest that a large amount of easily erodible till in the pathway of this flood allowed formation of such deposits. This is particularly significant as it indicates a relationship between the abundance of

coarse grained easily erodible material and the formation of depositional landforms. In regions of the Interior Plains where spillways do not coincide with thick packages of easily erodible material, this may explain the lack of depositional landforms.

Using our reconstruction of lake volume and peak discharge we can estimate the flood's duration. Based on the range of peak discharges, 14 000–26 000 m^3 s^{-1}, the 5.5 km^3 lake would have drained in between 3 and 5 days. The flood duration probably exceeds these values as peak discharge is unlikely to persist for the duration of drainage. Furthermore it is probable that continual drainage from Lake Algar would have sustained flow for much longer. However, these estimates provide a minimum assessment of the flood duration.

Wider deglacial significance

Based on the regional chronology of Dyke *et al.* (2003), the Beaver River Valley would have been deglaciated between 13.9 and 13.3 ka BP (12–11.5 ^{14}C ka BP). Therefore the region would have been ice free to allow the formation of the geomorphology and sedimentology described. We suggest that the timing of the flood falls between this age range. Furthermore, based on this age it is feasible that flood waters travelling down the Beaver River Spillway drained into Glacial Lake Meadow (Christiansen 1979; Schreiner 1983) potentially forming the delta recorded by Christiansen (1979). From here water was held in glacial Lake Meadow until the time the southwestern margin of the Laurentide Ice Sheet retreated allowing southeastern drainage of the lake through a complex of small spillways (Christiansen 1979; Schreiner 1983).

Significance of study

Well-preserved sedimentological evidence associated with glacial lake outburst floods, as discussed in this study, is exceedingly rare within the Interior Plains. This study therefore has several implications for the analysis and reconstruction of local hydraulic variables and for the controls on outburst flood erosional and depositional processes. Hydraulic calculations demonstrate the limitations of using palaeohydraulic equations based on sediment particle measurements. We suggest that such equations should be used with caution in locations where high sediment loads are likely, as such conditions limit the application of these methods of estimating velocity and peak discharge. This is particularly important as we demonstrate that within an outburst flood, with spatially variable sediment loads, landforms with similar geomorphic expression can be produced in hyperconcentrated and fluid flows, but with sedimentary characteristics that are dramatically different.

Furthermore, HEC-RAS derived peak discharge estimates show a significant increase in the lower part of the spillway. Based on observed outburst floods (Björnsson

1992; Kershaw *et al.* 2005) we would expect peak discharge to decrease in the spillway's lower reaches due to downstream discharge attenuation. While more work is required to fully understand the controls on outburst flood behaviour and hydraulics, these results demonstrate the importance of external controls such as sediment supply on outburst flood evolution. These inferences concur with observations made in modern settings (O'Connor *et al.* 2001; Breien *et al.* 2008), where outburst floods overtopping moraines have been rapidly hyperconcentrated or evolved into debris flows. However, the uniqueness of the flowpath of the Beaver River Spillway, travelling through a region of thick, easily erodible material, provided the opportunity to observe how a single flood event can exhibit a range of flow conditions, and associated sedimentological evidence.

Conclusions

We reconstruct the catastrophic drainage of glacial Lake Algar in north central Alberta based on the well-preserved sedimentary record within the eastern Beaver River Spillway. Based on regional deglacial chronology (Dyke *et al.* 2003), we suggest the flood occurred between 13.9 and 13.3 ka BP. We estimate the peak discharge of the flood using a HECgeoRAS/HEC-RAS model in conjunction with PSIs. Modelling results indicate that peak discharge within the first 40 km (Reach 1) of the eastern Beaver River Spillway was approximately 14 000–21 000 m^3 s^{-1}. Within the 120-km-long downstream reach (Reach 2), the peak discharge was estimated at 23 000–40 000 m^3 s^{-1} (n_{bulked} 18 000–26 000 m^3 s^{-1}). Based on lake volume estimates and the range of peak discharges from both reaches a minimum flood duration of 3–5 days is estimated. The downstream discharge increase coincides with a change in sediment composition of pendant bars. The increase in modelled peak discharge and compositional change of pendant bars occur downflow of the moraine barrier, which the spillway dissects. We suggest these changes, and increase in discharge estimates, result from sediment bulking of the flood flow due to the easily erodible nature of the moraine barrier, which produced differing hydraulics and associated sedimentology in close proximity from a single flood event.

Author contributions. – The project was conceived and designed by SLN and DGF. MM and DJU assisted with field sampling and interpretations. SLN wrote the manuscript with input from all authors.

References

Andriashek, L. D. & Fenton, M. M. 1989: *Quaternary Stratigraphy and Surficial Geology of the Sand River Area 73L.* Alberta Research Council, Edmonton.

Baker, V. R. 1973: Paleohydrology and sedimentology of Lake Missoula flooding in eastern Washington. *Geological Society of America Special Paper 144*, 1–79.

Beaney, C. L. 2002: Tunnel channels in southeast Alberta, Canada: evidence for catastrophic channelized drainage. *Quaternary International 90*, 67–74.

Björnsson, H. 1992: Jökulhlaups in Iceland: prediction, characteristics and simulation. *Annales of Glaciology 16*, 95–106.

Breien, H., De Blasio, F. V., Elverhoi, A. & Hoeg, K. 2008: Erosion and morphology of a debris flow caused by a glacial lake outburst flood, Western Norway. *Landslides 5*, 271–280.

Bretz, J. H., Smith, H. T. U. & Neff, G. E. 1956: Channeled scabland of Washington: new data and interpretations. *Geological Society of America Bulletin 67*, 957–1049.

Broecker, W. S., Kennett, J., Flower, B., Teller, J., Trumbore, S., Bonani, G. & Wolfli, W. 1989: Routing of meltwater from the Laurentide Ice Sheet during the Younger Dryas cold episode. *Nature 341*, 318–321.

Carling, P. A. 2013: Freshwater megaflood sedimentation: what can we learn about generic processes? *Earth-Science Reviews 125*, 87–113.

Carling, P., Villanueva, I., Herget, J., Wright, N., Borodavko, P. & Morvan, H. 2010: Unsteady 1D and 2D hydraulic models with ice dam break for Quaternary megaflood, Altai Mountains, southern Siberia. *Global and Planetary Change 70*, 24–34.

Christiansen, E. A. 1979: The Wisconsinan deglaciation, of southern Saskatchewan and adjacent areas. *Canadian Journal of Earth Sciences 16*, 913–938.

Clark, P. U., Marshall, S. J., Clarke, G. K. C., Hostetler, S. W., Licciardi, J. M. & Teller, J. T. 2001: Freshwater forcing of abrupt climate change during the last glaciation. *Science 293*, 283–287.

Costa, J. E. 1983: Paleohydraulic reconstruction of flash-flood peaks from boulder deposits in the Colorado Front Range. *Geological Society of America Bulletin 94*, 986–1004.

Costa, J. E. 1984: Physical geomorphology of debris flows. *In* Costa, J. E. & Fleisher, P. J. (eds.): *Developments and Applications of Geomorphology*, 268–317. Springer, New York.

Cutler, P. M., Colgan, P. M. & Mickelson, D. M. 2002: Sedimentologic evidence for outburst floods from the Laurentide Ice Sheet margin in Wisconsin, USA: implications for tunnel channel formation. *Quaternary International 90*, 23–40.

Dury, G. H. 1976: Discharge prediction, present and former, from channel dimensions. *Journal of Hydrology 30*, 219–245.

Dyke, A. S., Moore, A. & Robertson, L. 2003: Deglaciation of North America. *Geological Survey of Canada, Open File 1574*.

Ferguson, R. I. 1994: Critical discharge for entrainment of poorly sorted gravel. *Earth Surface Processes and Landforms 19*, 179–186.

Fisher, T. G. 1993: *Glacial Lake Agassiz: The N. W. outlet and paleoflood spillway, N. W. Saskatchewan and N. E. Alberta.* Ph.D. thesis, University of Calgary, 184 pp.

Fisher, T. G. & Lowell, T. V. 2017: Glacial geology and landforming events in the Fort McMurray region. *In* Ronaghan, B. (ed.): *Alberta's Lower Athabasca Plain: Archaeology and Paleoenvionments*, 45–68. Athabasca University Press, Alberta.

Fisher, T. G. & Smith, D. G. 1994: Glacial Lake Agassiz: its northwest maximum extent and outlet in Saskatchewan (Emerson phase). *Quaternary Science Reviews 13*, 845–858.

Fisher, T. G. & Taylor, L. D. 2002: Sedimentary and stratigraphic evidence for subglacial flooding south-central Michigan, USA. *Quaternary International 90*, 87–115.

Fisher, T. G., Smith, D. G. & Andrews, J. T. 2002: Preboreal oscillation caused by a glacial Lake Agassiz flood. *Quaternary Science Reviews 21*, 873–878.

Fisher, T. G., Waterson, N., Lowell, T. V. & Hajdas, I. 2009: Deglaciation ages and meltwater routing in the Fort McMurray region, northeastern Alberta and northwestern Saskatchewan, Canada. *Quaternary Science Reviews 28*, 1608–1624.

Herget, J. 2005: Reconstruction of ice-dammed lake outburst floods in the Altai Mountains, Siberia. *Geological Society of America, Special Paper 386,* 118 pp.

Horritt, M. S. & Bates, P. D. 2002: Evaluation of 1D and 2D numerical models for predicting river flood inundation. *Journal of Hydrology 268*, 87–99.

Hydrologic Engineering Center. 2001: HEC-RAS river analysis system. *Hydraulic Reference Manual version. 3.0. U.S. Army Corps of Engineering*. Davis, California. 46 pp.

Kehew, A. E. 1982: Catastrophic flood hypothesis for the origin of the Souris spillway, Saskatchewan and North Dakota. *Geological Society of America Bulletin 93*, 1051–1058.

Kehew, A. E. 1993: Glacial-lake outburst erosion of the Grand Valley, Michigan, and impacts on glacial lakes in the Lake Michigan Basin. *Quaternary Research 39*, 544–553.

Kehew, A. E. & Clayton, L. 1983: Late Wisconsinan floods and development of the Souris-Pembina spillway system in Saskatchewan, North Dakota and Manitoba. *In* Teller, J. T. & Clayton, L. (eds.): *Glacial Lake Agassiz*, 187–209. *Geological Association of Canada Special Paper 26*.

Kehew, A. E. & Lord, M. L. 1986: Origin and large-scale erosional features of glacial-lake spillways in the northern Great Plains. *Geological Society of America Bulletin 97*, 162–177.

Kehew, A. E. & Lord, M. L. 1987: Glacial-lake outbursts along the mid-continent margins of the Laurentide Ice Sheet. *In* Mayer, L. & Nash, D. (eds.): *Catastrophic Flooding*, 95–120. Allen and Unwin, London.

Kehew, A. E. & Teller, J. T. 1994: Glacial-lake spillway incision and deposition of a coarse-grained fan near Waterous, Saskatchewan. *Canadian Journal of Earth Science 31*, 544–553.

Kershaw, J. A., Clague, J. J. & Evans, S. G. 2005: Geomorphic and sedimentological signature of a two-phase outburst flood from moraine-dammed Queen Bess Lake, British Columbia, Canada. *Earth Surface Processes and Landforms 30*, 1–25.

Komar, P. D. 1987: Selective gravel entrainment and the empirical evaluation of flow competence. *Sedimentology 34*, 1165–1176.

Kozlowski, A. L., Kehew, A. E. & Brian, C. B. 2005: Outburst flood origin of the Central Kalamazoo River Valley, Michigan, USA. *Quaternary Science Reviews 24*, 2354–2375.

Lord, M. L. & Kehew, A. E. 1987: Sedimentology and paleohydrology of glacial-lake outburst deposits in southeastern Saskatchewan and northwestern North Dakota. *Geological Society of America Bulletin 99*, 663–673.

Maizels, J. K. 1991: Origin and evolution of Holocene sandurs in areas of Jökulhlaup drainage, south Iceland. *In* Maizels, J. K. & Caseldine, C. (eds.): *Environmental Change in Iceland: Past and Present*, 267–302. Kluwer, Dordrecht.

Maizels, J. 1997: Jökulhlaup deposits in proglacial areas. *Quaternary Science Reviews 16*, 793–819.

Malde, H. E. 1968: The catastrophic late Pleistocene Bonneville flood in the Snake River Plain, Idaho. *US Geological Survey Professional Paper*, 595 pp.

Margold, M., Jansen, J. D., Codilean, A. T., Preusser, F., Gurinov, A. L., Fujioka, T. & Fink, D. 2018: Repeated megafloods from glacial Lake Vitim, Siberia, to the Arctic Ocean over the past 60,000 years. *Quaternary Science Reviews 187*, 41–61.

Munro-Stasiuk, M. J. 1999: Evidence for water storage and drainage at the base of the Laurentide ice sheet, south-central Alberta, Canada. *Annals of Glaciology 28*, 175–180.

O'Connor, J. E. 1993: Hydrology, hydraulics, and geomorphology of the Bonneville Flood. *Geological Society of America Special Paper 274*, 83–89.

O'Connor, J. E., Hardison, J. H. & Costa, J. E. 2001: Debris flows from failures of Neoglacial-age moraines in the Three Sisters and Mount Jefferson wilderness areas, Oregon. *US Geological Survey Professional Paper 1606*.

Parker, G. 1990: Surface-based bedload transport relation for gravel rivers. *Journal of Hydraulic Research 28*, 417–436.

Pierson, T. C. 1981: Dominant particle support mechanisms in debris flows at Mt. Thomas, New Zealand, and implications for flow mobility. *Sedimentology 28*, 4940–4953.

Russell, A. J., Roberts, M. J., Fay, H., Marren, P. M., Cassidy, N. J., Tweed, F. S. & Harris, T. 2006: Icelandic jökulhlaup impacts: implications for ice-sheet hydrology, sediment transfer and geomorphology. *Geomorphology 75*, 33–64.

Schreiner, B. T. 1983: Lake Agassiz in Saskatchewan. *In* Teller, J. T. & Clayton, L. (eds.): *Glacial Lake Agassiz*, 75–96. Geological Association of Canada Special Paper 25.

Sjogren, D. B. & Rains, R. B. 1995: Glaciofluvial erosional morphology and sediments of the Coronation-Spondin Scabland, east-central Alberta. *Canadian Journal of Earth Sciences 32*, 565–578.

Smith, G. A. 1986: Coarse-grained nonmarine volcaniclastic sediment: terminology and depositional Processes. *Geological Society of America Bulletin 97*, 1–10.

Teller, J. T., Leverington, D. W. & Mann, J. D. 2002: Freshwater outbursts to the oceans from glacial Lake Agassiz and their role in climate change during the last deglaciation. *Quaternary Science Reviews 21*, 879–887.

Thompson, S. M. & Campbell, P. L. 1979: Hydraulics of a large channel paved with boulders. *Journal of Hydraulic Research 17*, 341–354.

Todd, S. P. 1989: Stream-driven, high-density gravelly traction carpets: possible deposits in the Trabeg Conglomerate Formation, SW Ireland and some theoretical considerations of their origin. *Sedimentology 36*, 513–530.

Travis, B., Teal, M. & Gusman, J. 2012: Best Methods and Inherent Limitations of Bulked Flow Modeling with HEC-RAS. *Conference Proceedings of the 2012 World Environmental and Water Resources Conference*, 1–8. Albuquerque, New Mexico.

Utting, D. J., Atkinson, N. & Pawley, S. 2015: Reconstruction of proglacial lakes in Alberta. *Canadian Quaternary Association Conference*, program with abstracts p.82. St. John's, Canada.

Waitt, R. B. 1980: About 40 last-glacial Lake Missoula Jökulhlaups through southern Washington. *Journal of Geology 88*, 653–679.

Waitt, R. B. 1985: Case for periodic, colossal jökulhlaups from glacial Lake Missoula. *Geological Society of America Bulletin 95*, 1271–1286.

Williams, G. P. 1983: Paleohydrological methods and some examples from Swedish fluvial environments I: cobble and boulder deposits. *Geografiska Annaler 65*, 227–243.